ISSN: 2230-9926

Available online at http://www.journalijdr.com

IJDR

International Journal of Development Research
Vol. 12, Issue, 03, pp. 54720-54734, March, 2022
https://doi.org/10.37118/ijdr.24126.03.2022

RESEARCH ARTICLE OPEN ACCESS

PROPOSED METHODOLOGY FOR ANALYSIS OF HARMONIC IMPACTS IN ELECTRICAL GRIDS USING DECISION TREE TECHNIQUE - PART 1

Pedro Ferreira da Silva Filho*[1], Jandecy Cabral Leite[1,2] and Rivanildo Duarte Almeida[2]

[1.2]Postgraduate Master's Degree in Process Engineering at the Institute of Technology of the Federal University of Pará (PPGEP/ITEC/UFPA). Avenida Augusto Correia, nº 01. Guamá. Belém-Pará, Brazil. ZIP CODE: 66.075-110 Instituto de Tecnologia e Educação da Amazônia; [2]Galileo (ITEGAM). Joaquim Nabuco Avenue, No. 1950. Downtown. Manaus - Amazonas, Brazil. ZIP CODE: 69020-030.

ARTICLE INFO

Article History:
Received 20th January, 2022
Received in revised form
26th January, 2022
Accepted 11th February, 2022
Published online 28th March, 2022

Key Words:
Methodology, Harmonic Impacts, Electrical Networks, Computational Intelligence, Decision Tree.

Corresponding author:
Pedro Ferreira da Silva Filho,

ABSTRACT

The progressive use of power electronic devices, connected to the electrical system, has contributed to the increase of problems caused by harmonic disturbances in electrical networks. Thus, this work aims to develop a methodology to analyze the harmonic impacts on the electrical grids caused by non-linear loads with the use of the Decision Tree technique. The model used was the regression tree through the use of the Classification and Regression Tree (CART) algorithm, which relates the harmonic current of a non-linear load and the harmonic voltage at the common connection point of the electrical grid. The technique used was applied in a case study in order to show the validity of its application in solving problems that seek to investigate the dependency relationship between the two variables. Among the feeders used in the research for the 3rd harmonic analysis, feeder DIAL2-19 contributed the impact factor for phase A with 43.587%. The feeder DIAL2-16 contributed with impact factor 36.407% for phase B. For phase C feeder DIAL2-17 contributed 26.434% impact factor.

Citation: ***Pedro Ferreira da Silva Filho, Jandecy Cabral Leite and Rivanildo Duarte Almeida.*** "Proposed methodology for analysis of harmonic impacts in electrical grids using decision tree technique - part 1*", International Journal of Development Research*, 12, (03), 54720-54734.

INTRODUCTION

Electric Power Quality (QPE) has become a problem with obstacles since electric power was discovered, becoming an area of great interest in recent years due to the insertion of new electrical/electronic appliances in the market that connect to the power grid, and import an electric current from the power supply network, which flows through the impedances of the power supply system causing a voltage drop, which affects the voltage supplied to the customer (KUMAR AND ALEXANDER, 2019). Power quality is defined based on four important measurements of electrical parameters, namely voltage, current, frequency, and phase; therefore, both voltage and current must be in sinusoidal form with specified magnitude at a constant frequency without any phase shift (ZOBAA AND ALEEM, 2017). Nonlinear loads are sources of harmonic currents that contaminate the electrical system with disturbances such as distortion in the voltage waveform (SOUZA *et al*., 2021).The presence of nonlinear loads in power grids contributes to change the characteristics of voltage and current waveforms in power systems, which differ from constant amplitude signals with pure sinusoidal, therefore, advanced signal processing techniques are required for accurate measurement of the electrical quantities of voltage, current, frequency and phase of the power system. The impact of nonlinear loads on power electrical systems has increased in recent decades, thus introducing non-sinusoidal current consumption patterns (current harmonics), which can be found in circuits for motor drives, electronic reactors for discharge lamps, personal computers, or electrical appliances (SOLIMAN AND ALKANDARI, 2011). The presence of voltage and current waveform distortion is usually expressed in terms of harmonic frequencies that are integral multiples of the power system's nominal frequency. It is a constant phenomenon in a power system and is completely different from transient distortion results, such as faults, in a power system (SOLIMAN AND ALAMMARI, 2013). To improve power quality, knowledge of the source of harmonics, voltage disturbances, and waveform interruptions is essential (ULLAH *et al*., 2019). The most common solution to the harmonic distortion problem is based on the application of passive filters. Before implementing the solution, it is necessary to identify the main sources of harmonics in an electrical system and know the percentage contribution of each source, in order to more effectively solve the problem (ALMEIDA AND LEITE, 2018). Therefore, it is necessary to identify, measure the levels of harmonic distortions in the electrical system and identify

in which feeders or points there is the greatest contribution in harmonic distortions. This identification aims to discover the sources of harmful harmonics to the electrical system, for the best decision making in solving this problem. This work uses a computational intelligence technique called Decision Tree, to identify and measure the harmonic impacts caused by the injection of harmonic currents generated by non-linear loads. The technique used seeks a correlation between injected harmonic current and the harmonic voltage at the electrical system bar, thus identifying where there is the greatest contribution of harmonic sources. With the intention of maintaining the harmonious coexistence between disturbing equipment and sensitive equipment, it is necessary to establish limits and standards for controlling such deeds or phenomena. The standards are: Institute of Electrical and Electronics Engineers (IEEE STD 519 - 2014), in the United States, International Electrotechnical commission (IEC 61000-3-6), in Europe and Procedimentos de Distribuição de Energia Elétrica no Sistema Elétrico Nacional (PRODIST - MÓDULO 8), in Brazil. This work contributes not only to the incentive of the creation of normative documents that attribute responsibilities about harmonic distortion limit violations, but also to the stimulus of the inclusion in the electric energy tariffs the implications of the harmonic content of the loads that pollute the feeding system. In recent years, the increasing use of power electronic devices in electrical systems has led to more and more problems related to harmonic disturbances or distortions in electrical networks. This phenomenon affects all industrial (use of dimmers, rectifiers, variable speed drives, speed), tertiary (computer or office lighting, retail, ...) and domestic (TVs, household appliances, ...) sectors (KAMEL *et al*., 2018). Harmonic distortion is generated by nonlinear loads connected to the power grid and absorbing non-sinusoidal currents. These current harmonics will in turn generate harmonic voltages at different grid connection points. For the other electrical equipment connected at these points, this harmonic pollution has detrimental effects, for example: the deformation of the grid voltage waveform at the common connection point (CCP), heating of cables and electrical equipment, sudden stoppage of rotating machines, while the power utility is obliged to provide clean power (GOPAL and YARNAGULA, 2014). The present research is relevant due to the need to measure and identify the levels of harmonic distortions, the impacts on the electrical network, and then propose solutions that can minimize the impacts caused in the electrical network, among which we can also mention:

a) Overload in the electrical systems due to the increase of the effective current;
b) Overload in the neutral conductors due to the 3rd order harmonic currents;
c) Heating, vibrations and aging of alternators, transformers and motors;
d) Heating and aging of reactive power compensation capacitors;
e) False performance of sensors and protection equipment;
f) Burning or inadequate operation of sensitive equipment;
g) Disturbance in communication networks or telephone lines;
h) Measurement errors.

This research has as its contribution the practical application of a valid methodology through case studies for harmonic impact analysis considering the recommendations of IEC 61000-3-6 (IEC/TR, 2008-02), IEEE Std. 519-2014 and PRODIST/MODULO 8/ANEEL, revision year 2021, that serves as a base and support material for more advanced research on harmonic distortion and power quality as a whole.

LITERATURE REVIEW

Basics of Harmonic Distortion and Power Quality: With society's need to avoid wasting electricity and for equipment to have a good working condition, utilities have been concerned about the quality of power (QE) supplied to their customers. The definition of power quality for IEEE-1159 (2019) is the wide variety of electromagnetic phenomena occurring in the power grid at a given time and
place that characterize voltage and current; these measurements are compared to ideal or acceptable values (BELEIU, 2018). While for authors KAVITHA and SUBRAMANIAN (2017) point out that power quality is the set of the entire power grid satisfactorily operate an equipment without having continuous loss of life of all other equipment. For TRIPATHI (2016) power quality is related to changes and disturbances in the supplied electrical power that can produce failures and malfunctions of electrical and electronic equipment. Despite the lack of consensus we can define power quality as the characterization of the current and voltage of the electric network and compare them with acceptable values; these values should cause other equipment connected to the network to work properly and not produce changes, disturbances, nor produce failures in electrical and electronic equipment. The disturbance that most affects the quality of power is harmonic distortion. The power electric system (SEP), through the utilities, aims to provide consumers with electrical energy safely, reliably, and with quality (BAYINDIR, 2016, CARDOSO and HOFFMANN, 2019). This supplied power should be distortion-free, fully sinusoidal (BELE and GHUTKE, 2019, DHANDE and PATHAN, 2019); but the progressive increase in these distortions has caused concerns to the suppliers and customers of this power (JOHNSON and HASSAN, 2016, WANG, 2016). These signal distortions in the power grid are known as harmonic distortions (JAYASINGHE, 2017). Harmonic distortion are deformations, distortions or removal of compatibility of the sine wave of the current and voltage of the power grid (SILVA *et al*., 2016). While for LOPEZ (2016), highlights these distortions as harmonic disturbances that also affect the voltage and current; these distortions are consequences of several sine waves added where their frequencies are integer proportions of the fundamental, these waves are called harmonics. Author ALEXANDER (2016) defines harmonic distortions as the deviation of the frequency of an ideal sine wave from the value of the source frequency, this is characterized through the spectral content presented with the deviation. It can be stated that harmonic distortions are harmonic disturbances that affect the voltage and current of the power grid; so as to distort and deform the source sinusoidal signal; and can be characterized by multiple sine waves multiple integer values of the fundamental frequency and the spectral content presented.

The multiple sine waves or grouping of the fundamental wave and its components or the set of possible modes of oscillation is called harmonic series (PATEL *et al*., 2020, KOLMAKOV, 2020, HALLIDAY *et al*., 2016). This series is formed by sine waves composed of the fundamental frequency (f) and other frequencies that are integer multiples (2f, 3f, 4f, ...) of it (KERBER and ESTEVES, 2018). Thus one can define the harmonic series as the grouping of harmonic components formed by sine waves that has a fundamental frequency (f) and integer multiples of this (2f, 3f, 4f, ...). Among the modes of oscillation, the fundamental mode, or fundamental frequency, or first harmonic is the one with the lowest frequency. The other modes of oscillation are: second harmonic, third harmonic and so on (HALLIDAY, 2016). For Carvalho (2018) the first wave is known as the fundamental wave. According to IEEE Std 1453 (2015), the fundamental frequency is the reference frequency for the others that are originated from the Fourier transform of a function in time. This function with respect to time had the same frequency as the fundamental. It is noteworthy that the fundamental frequency is also called the first harmonic or fundamental mode. It is defined as the frequency generated by the Fourier series that works as a reference for the other waves generated, it is the frequency of the function, the smallest, or the first wave of the oscillation modes.

The existence of the harmonic distortions at a common coupling point (CAP) occurs due to the harmonic sources in the distribution system and in the consumer network (SALEHI *et al*., 2019, PAPIČ *et al*., 2018). For the authors RASUL *et al*. (2017) and RANI *et al*. (2016) the main sources of harmonic current consumption are the nonlinear loads or devices with these characteristics in the electrical system. The nonlinear loads connected to the electrical system produce harmonics that contaminate the electrical grid and cause harmful effects to the power system and these distortions are of currents and voltages (JAISIVA *et al*., 2016). The grid voltage when applied to a nonlinear load, it injects a current that distorts the applied voltage

(RANI *et al*, 2016). Besides nonlinear loads another cause of harmonic distortions are renewable energy generators that use cycloconverters and inverters in photovoltaic and wind generation (BECKER *et al*., 2016, JEDRZEJCZAK, 2016). For further clarification, in the following sub-items the linear and non-linear loads are presented, given that electricity consumers use these loads connected to the power system (FRANCHI, 2017.)

Linear Loads: For authors DA SILVEIRA and his collaborators (2018) in conjunction with OLIVEIRA (2018), highlight that linear loads are formed by resistances, inductances, and capacitances. They also state that the format of the voltage and current waveforms are the same, that is, they are signals without deformation relative to each other and with the same given frequency. These waveforms may be in phase in the case of a resistive load; the voltage may be leading in the case of an inductive load; or the voltage may be lagging in the case of a capacitive load; but in all cases the current and voltage waveforms are sinusoidal. Figure 1(a) shows the electric circuit of the grid connected to a resistive load and Figure 1(b) shows the waveforms of the current and voltage that are in phase. For FORTES (2018) current and voltage are proportional to each other for a given frequency, the equation that describes this relationship is given by Eq. (1).

$$v(t) = R \cdot i(t) \quad (1)$$

Where:
v(t) = mains voltage
i(t) = mains current
R = Resistance of the load

The current and voltage have the same format of the applied signal for a given frequency; these signals can be offset due to an inductance or a capacitance, but what characterizes them as linear is that both have the same signal format, sinusoidal, in the case of the grid.

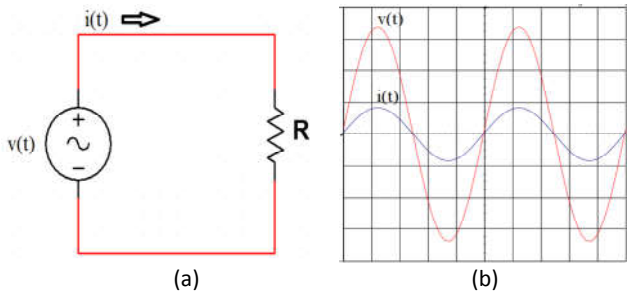

Figure 1. Power grid connected to a resistive load in (a); and in (b) the waveforms of the current and voltage in phase

Figure 2 shows an example of a linear (inductive) load connected to the grid with the current and voltage signals shown. The electrical circuit is highlighted in Figure 2(a) and the waveforms in Figure 2(b). The current and voltage signals are sinusoidal and offset from each other. The voltage is in phase ahead of the current and it can be seen that they are not deformed, which characterizes a linear load. A linear load, when connected to the electrical grid, demands from the grid a current that is not deformed, that is, the current is sinusoidal. This current coming from the PAC interacts with the grid impedance that is also linear, so it will not produce other voltages that could distort the grid voltage (KULLARKAR *et al*., 2017). As an example of linear loads we have: Electric shower, induction motors, incandescent lamps, heaters, capacitor bank for power factor correction, filter capacitors (KULLARKAR *et al*., 2017, MIKKILI and PANDA, 2018).

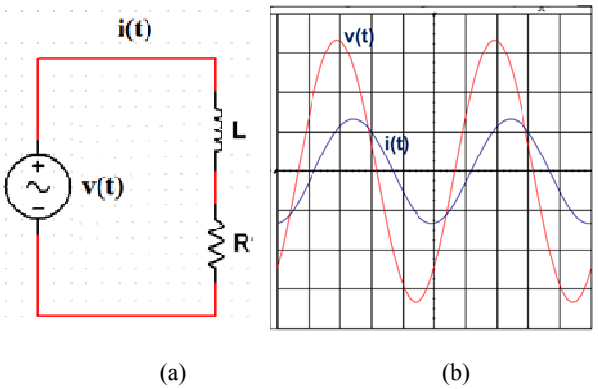

Figure 2. Linear load connected to the electrical grid (a); voltage and current signals offset (b)

Linear loads do not present problems for the quality of electric power, because they do not produce harmonic distortions in the current or voltage. There is another type of load that brings serious concerns to the suppliers and consumers of electrical power, the non-linear loads.

Non-Linear Loads: Loads composed of the following components: resistors, capacitors and inductors, when subjected to power controls this whole set is known as non-linear loads (WATEGAONKAR *et al*., 2018, DESAI *et al*., 2016). Nonlinear loads are those that when subjected to a sinusoidal voltage source it requests a non-sinusoidal current from the source (IEEE Std. 519-2014, MOTTA and FAÚNDES, 2016, MILANI, 2017). These loads generate harmonic currents that deform the current signal and as a consequence produce harmonic voltage drops; these deformed voltages reach and affect the power grid in a way that produces disturbances and with this cause problems in other equipment connected to it (DE LEON II *et al*., 2017, FRANCHI, 2017). Figure 3 shows the waveforms of the mains voltage (a) and current (b) at the input of a bridge rectifier of a power supply that uses components based on power electronics. One can observe the deformation of the current in relation to the sinusoidal grid voltage. With the increasing advancement of power electronics, there was also an increase in the amount of semiconductor devices that allowed for more efficient and more economical equipment (KO and GU, 2016, BELTRAN-CARBAJAL and SILVA-NAVARRO, 2017, SILVA *et al*., 2019). Semiconductor manufacturing was seen as a promising investment with positive returns to reduce power quality problems (DE LEON II *et al*., 2017). Quality has improved, but the use of these devices has significantly increased nonlinear loads in the system (SILVA *et al*., 2019, WATEGAONKAR *et al*., 2018). These loads produce harmonics that are generated due to the switching that these devices do with the grid signal (SAAD *et al*., 2017, YANG *et al*., 2016).

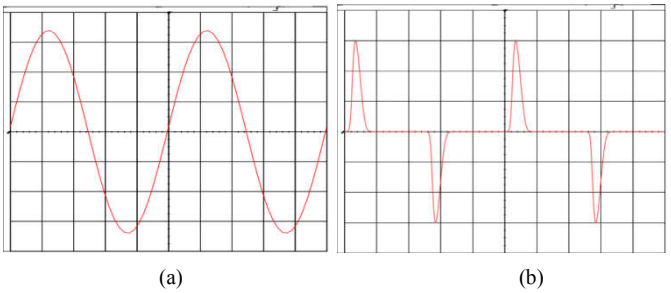

Figure 3. Waveform of the mains voltage (a); waveform of the current requested from the source at the input of an equipment based on power electronics

As examples of semiconductor components used for current commutation, we can highlight: the diode, bipolar junction transistor, MOSFET, IGBT, SCR and TRIAC. The equipment where these components are used are: switching sources, LED light fixtures, televisions (DIONISIO and SPALDING, 2016), converters, inverters, adjustable speed inverters (WATEGAONKAR *et al*., 2018), washing

machine, battery charger, computers (KUMAR and ZARE, 2015). There are other equipment that are not the basis of power electronics but also produce harmonics among them are the arc devices which are: fluorescent and compact lamps (CHAKRAVORTY, 2016, MEYER, 2016), arc furnace (SEZGIN and SALOR, 2019, WATEGAONKAR *et al*., 2018) and welding machine (JEDRZEJCZAK, 2016, MANUSOV and KHRIPKOV, 2018). It is observed that harmonics are produced through various equipment, either power electronics based or not that are found in various sectors of our society, these equipment are nonlinear loads that produce the distortion of current in the power grid. A non-linear load connected to the electrical grid absorbs from it a harmonic current that reaches the common coupling point (CAP); this is a deformed current compared to the voltage that fed it. The harmonic voltage arises from the impedance of the grid as the harmonic current passes through it. Each harmonic component of the current with its appropriate frequency and amplitude produces, as it flows through the grid impedance, a component for the harmonic voltage. Every set of the current components will produce a set of harmonic components of the voltage that will cause the grid voltage to be deformed (STIEGLER, 2015, RANI *et al*., 2016, SILVA *et al*., 2019). For MONTEIRO (2017) the definition of the harmonic impedance of the power grid is given by the relationship between the voltage and the current for a given Measurement Point (MP), according to Eq. (2).

$$Z_{MP}(f) = \frac{V_{MP}(f)}{I_{MP}(f)} \quad (2)$$

Where: $V_{MP}(f)$ e $I_{MP}(f)$ are, respectively, the voltages and currents obtained from the Fourier Transform for frequency f.

The connection between the currents emitted by the several equipments connected to the electrical grid (at the common coupling point - PAC), and the harmonic voltage levels in the grid is the harmonic impedance. Knowing the value of this impedance is of fundamental importance to know the propagation and level of harmonics emitted in the electrical grid. With the identification of these harmonics it is possible to establish the limits so that there is perfect compatibility among the several equipments connected to the electrical grid. If this compatibility is not adequate the harmonics produced can disturb or damage other loads connected to the PAC (STIEGLER, 2015, CHAKRAVORTY, 2016, RANI *et al*., 2016,).
A deformed signal, either of current or voltage, can be represented by several harmonics, with their respective amplitudes and frequencies. This representation is used for analysis and study purposes to guide on the best strategy for the reduction of harmonics. The distorted signal can be represented by Fourier series.

Fourier Series: We can find various periodic waveforms: triangular, square, sawtooth; these waves are not represented by a cosine or sine function. Functions of this type are called non-sine waves. Periodic waves are those that repeat themselves cyclically, and are found in many pieces of electronic equipment. The electric power system has periodic sine waves generated by the power plants that feed the loads.
At the common coupling point there are also non-sinusoidal periodic waves that are distorted waves, which are harmful to the electrical system. To find methods for removing or reducing these inconvenient signals it is necessary to know them. The way used to quantify this type of signal in the form of amplitude and lag for each specific frequency is through Fourier series (SEITHTANABUTARA *et al*., 2020, SANG, 2016). The Fourier series is also used to represent small non-periodic signals, where these signals have a finite period. For non-sinusoidal and non-continuous waves their representation is done by the Fourier transform (NAHVI and EDMINISTER, 2018, LV *et al*., 2018). The Fourier series known after the mathematician who formulated it, Jean Baptiste Fourier, is the representation of a periodic function by the summation of sine functions whose frequencies are multiples of the frequency of the analyzed signal, that is, the fundamental frequency (SAGGIO, 2019, OZDEMIR, 2021). A function is said to be periodic when it repeats at each cycle of the signal, so f(t) to be periodic, satisfies the equation f(t) = f(t + nT), where T is the period of the function (positive value) and n an integer ($n \geq 1$). Equality of Equation (3) is possible only if the series converges to the function f(t). For this, some criteria should be observed before asserting equality. It was established by Dirichlet conditions for convergence for the Fourier series. These conditions are (NAHVI and EDMINISTER, 2018, LANCZOS and BOYD, 2016):

(i) The function f(t) must be definite and unique, but in the possibility that it is discontinuous there will be, during the period of the function, a finite number of discontinuities.
(ii) The function must be periodic of period T;
(iii) During the interval -T/2 and T/2 the function has a mean value

For DAS (2015) the trigonometric Fourier Series for a periodic function f(t) as a function of time is presented in Equation (3). For SEROV (2017) every value of t in the Fourier series converges to the function f(t) quoted.

$$f(t) = a_0 + \sum_{n=1}^{\infty}[a_n \cos\left(\frac{2\pi nt}{T}\right) + b_n \sin(\frac{2\pi nt}{T})] \quad (3)$$

Where:

a_0= mean value or DC component of the function for one complete cycle;
a_n= coefficient of the series, is a rectangular component of the nth harmonic;
b_n= coefficient of the series, is a rectangular component of the nth harmonic;
n = nth harmonic, number of the harmonic;

In Equations (4), (5) and (6), the equations for calculating a0, an and bn, respectively, are presented:

$$a_0 = \frac{1}{T}\int_{-T/2}^{T/2} f(t)\,dt \quad (4)$$

$$a_n = \frac{2}{T}\int_{-T/2}^{T/2} f(t)\cos\left(\frac{2\pi nt}{T}\right)dt \quad \text{(para n = 1, 2, ..., } \infty) \quad (5)$$

$$b_n = \frac{2}{T}\int_{-T/2}^{T/2} f(t)\sin\left(\frac{2\pi nt}{T}\right)dt \quad \text{(para n = 1, 2, ..., } \infty) \quad (6)$$

The above equations which are expressed as a function of time, ask to be written as a function of frequency ω (fundamental frequency), by replacing $\omega=2\pi/T$. Equations (7), (8) and (9) are expressed as a function of frequency:

$$a_0 = \frac{1}{2\pi}\int_{-\pi}^{\pi} f(\omega t)d(\omega t) \quad (7)$$

$$a_n = \frac{1}{\pi}\int_{-\pi}^{\pi} f(\omega t)\cos(n\omega t)d(\omega t) \quad (8)$$

$$b_n = \frac{1}{\pi}\int_{-\pi}^{\pi} f(\omega t)\sin(n\omega t)d(\omega t) \quad (9)$$

Equation (3) when transformed from a function of time to a function of angular frequency, we have:

$$f(t) = a_0 + \sum_{n=1}^{\infty}[a_n \cos(n\omega t) + b_n \sin(n\omega t)] \quad (10)$$

Equation (10) can be written in terms of sine or cosine, amplitude, and with the phase angle of the harmonics (NILSSON, 2020, DAS, 2015), according to Equation (11) and (12).

$$f(t) = a_0 + \sum c_n \cos(n\omega t - \theta_n) \quad (11)$$

$$f(t) = a_0 + \sum c_n \sin(n\omega t + \phi_n) \quad (12)$$

$$c_n = \sqrt{a_n^2 + b_n^2} \quad (13)$$

$$\theta_n = tg^{-1}\left(\frac{b_n}{a_n}\right) \quad (14)$$

$$\phi_n = tg^{-1}\left(\frac{a_n}{b_n}\right) \quad (15)$$

The terms in the equation are:

a_0= DC component of the function (average);
c_n= amplitude of the phasor of the n-th harmonic;
$n\omega$= nth harmonic;
θ_n= lag angle of the n-th harmonic component for the cosine function;
ϕ_n= lag angle of the nth component of the harmonic for the sine function;

In Equation (16) the Fourier series grating in polar form is presented in equality with the rectangular form. This equation in polar form highlights the amplitude (An) with the due lag of the angle of the frequency of the nth harmonic, ϕ_n.

$$A_n\angle\phi_n = a_n + jb_n \quad (16)$$

The term in Equation (10) described with the cosine and sine function are highlighted in Equations (17) and (18), respectively.

$$a_n \cos(n\omega t) + \mathrm{b_n} \sin(n\omega t) = c_n \cos(n\omega t - \theta_n) = A_n\angle - \theta_n = a_n - jb_n \quad (17)$$

$$a_n \cos(n\omega t) + \mathrm{b_n} \sin(n\omega t) = c_n \operatorname{sen}(n\omega t + \phi_n) = A_n\angle\theta_n = a_n + jb_n \quad (18)$$

In addition to the trigonometric form the Fourier series can be written in exponential form, for this the Euler identity in Equation (19) is applied to the trigonometric Fourier series in addition to Equation (20).

$$e^{i\theta} = cos\theta + isin\theta, \qquad e^{-i\theta} = cos\theta - isin\theta \quad (19)$$

$$\cos\theta = \frac{e^{i\theta}+e^{-i\theta}}{2} e \operatorname{sen}\theta = \frac{e^{i\theta}-e^{-i\theta}}{2i} \quad (20)$$

This gives the Fourier series equation as described in Equation (21).

$$\mathrm{f(t)} = \frac{a_0}{2} + \frac{1}{2}\sum_{n=1}^{n=\infty}(a_n - j\,b_n)e^{jn\omega t} + \frac{1}{2}\sum_{n=1}^{n=\infty} a_n - jb_n)e^{-jn\omega t} \quad (21)$$

After the mathematical development the new function for the Fourier series becomes that of Equation (22), the Fourier series of exponential form.

$$\mathrm{f(t)} = \frac{a_0}{2} + \frac{1}{2}\sum_{n=-\infty}^{n=\infty}(a_n - j\,b_n)e^{jn\omega t} \quad (22)$$

Equation (23) shows the Fourier series in complex form, and Equation (24) highlights cn which is a complex magnitude, where n = 0, ±1, ±2, ...

$$\mathrm{f(t)} = \sum_{n=-\infty}^{\infty} c_n\, e^{jn\omega t} \quad (23)$$

$$c_n = \frac{1}{2}(a_n - jb_n) = \frac{1}{T}\sum_{-T/2}^{T/2} f(t)\, e^{-jn\omega t} dt \quad (24)$$

To determine the Fourier series either in trigonometric form, or as a function of frequency or in complex form, it is necessary to calculate a0, an and bn which take a lot of time, if the effect of symmetry of the waveform is not observed. There are four symmetries that will facilitate the calculations when determining the Fourier series. They are the symmetries: of the even, odd, half-wave, and quarter-wave functions (DAS, 2015). When a function is axis symmetric and has a waveform on the right side of the axis, equal to that on the left side (mirror image of the other) during the interval from -T/2 to T/2 and satisfies Equation (25), the function is even.

$$f(-t) = -f(t) \quad (25)$$

In Figure 4 is vizualized even periodic function, it can be observed that the waveform in the time interval from 0 to T/2, has a mirror from -T/2 to 0; for the frequency function T=2π.

For the even function, Equations (7), (8), and (9) are reduced in difficulty, as shown in Equations (26), (27), and (28), respectively.

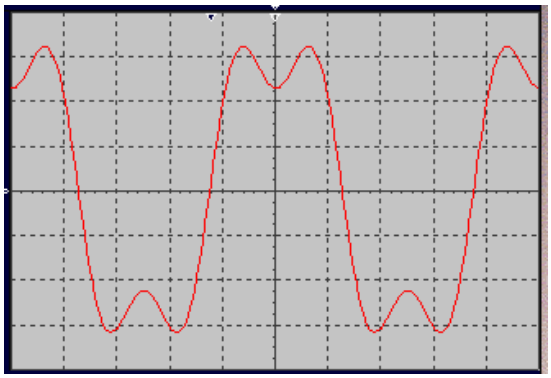

Figure 4. Even periodic function

$$a_0 = \frac{1}{2\pi}\int_{-\pi}^{\pi} f(\omega t)d(\omega t) \quad (26)$$

$$a_n = \frac{1}{\pi}\int_{-\pi}^{\pi} f(\omega t)\cos(n\omega t)d(\omega t) \quad (27)$$

$$b_n = 0, \text{ para todo n} \quad (28)$$

The average value of the area occupied by the graph during the interval is the sum of the areas for the period. It can be observed that in the even function all values of bn are zero, so in the Fourier series you will have only the cosine function.

The function is odd when it satisfies Equation (29).

$$f(t) = -f(-t) \quad (29)$$

For the odd function, Equations (7), (8), and (9) are reduced in difficulty according to Equations (30), (31), and (32), respectively.

$$a_0 = 0 \quad (30)$$

$$a_n = 0 \text{ para todo n;} \quad (31)$$

$$b_n = \frac{1}{\pi}\int_{-\pi}^{\pi} f(\omega t)\sin(n\omega t)\, d(\omega t) \quad (32)$$

When developing the coefficients of the Fourier series, it is observed that the sum of the areas on each side of the axis is zero (a0 = 0), that is, the mean. In the series the cosine function does not appear (an =0) only the sine function is present.

Figure 5 shows a non-sinusoidal waveform with symmetry on the zero axis of an odd function. In the interval from -T/2 to 0 the area of the figure is negative and from the interval from 0 to T/2 the area is positive; the sum of the two areas is the mean value (ao). For the frequency domain T = 2π.

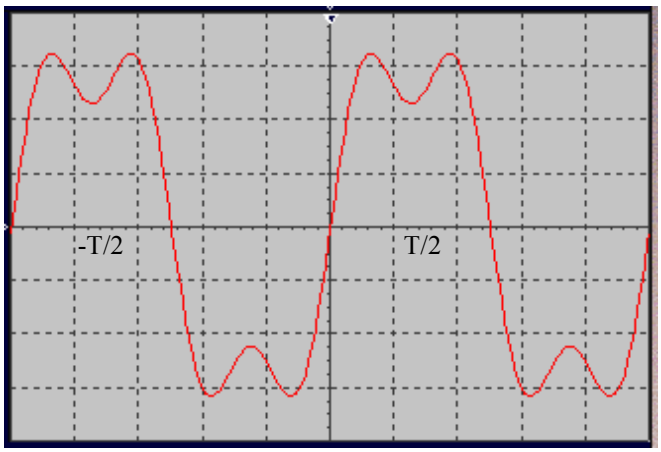

Figure 5. Symmetric non-sinusoidal waveform of an odd function

For the same graph we can have an even or an odd function, just move the axis, this can be observed in figures 4 and 5.

For half-wave symmetry the periodic function obeys Equation (33).

$$f(t) = -f\left(t - \frac{T}{2}\right) \quad (33)$$

In Figure 6 the waveform with half-wave symmetry is visualized. It can be seen that after half a period of displacement of the function and reversed it returns to the function of before.

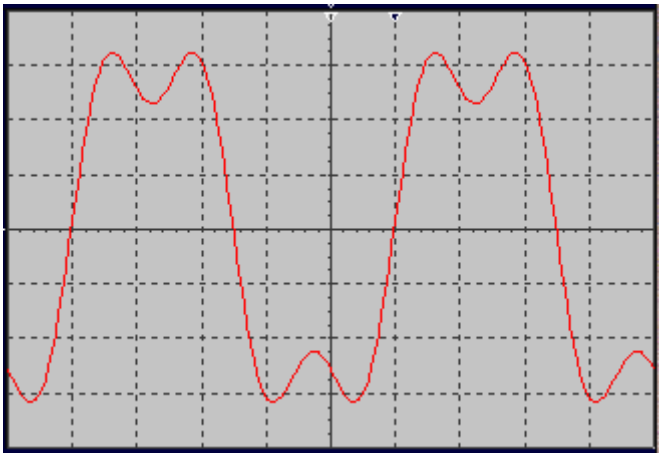

Figure 6. Waveform with half-wave symmetry

The waveforms in Figures (4) to (6) are also waveforms with half-wave symmetry. By developing the coefficients of the Fourier series, Equation (7), (8) and (9), for the function with half-wave symmetry, we obtain equations (34), (35), (36), (37) and (38).

$$a_0 = 0 \quad (34)$$

$$a_n = 0 \quad \text{for even n;} \quad (35)$$

$$a_n = \frac{1}{\pi}\int_{-\pi}^{\pi} f(\omega t)\cos(n\omega t)d(\omega t) \text{for odd n;} \quad (36)$$

$$b_n = 0 \quad \text{for even n;} \quad (37)$$

$$b_n = \frac{1}{\pi}\int_{-\pi}^{\pi} f(\omega t)\sin(n\omega t)d(\omega t) \text{ for odd n;} \quad (38)$$

For the half-wave symmetry function in the Fourier series the mean value of the function is zero and it has only odd harmonics. The function with quarter-wave symmetry is symmetric with respect to half of each semicycle of the wave and symmetric at each half-wave. Figure 7 shows the waveform for the function with quarter-wave symmetry. The components of the Fourier series for the function with quarter-wave symmetry are presented when they are transformed into even or odd. When they are even they are presented in Equations (39), (40), (41), and (42).

$$a_0 = 0, \text{ due to the half-wave symmetry} \quad (39)$$

$$a_n = \frac{2}{\pi}\int_{-\pi}^{\pi} f(t)\cos(n\omega t)d(\omega t), \text{for odd n} \quad (40)$$

$$a_n = 0, \text{ for all n, due to half-wave symmetry} \quad (41)$$

$$b_n = 0, \text{ for all n, because the function is even} \quad (42)$$

The function with quarter-wave symmetry when it is odd are shown in Equations (43), (44), (45) and (46).

$$a_0 = 0, \text{because the function is odd} \quad (43)$$

$$a_n = 0, \text{for all n, because the function is odd} \quad (44)$$

$$b_n = 0, \text{ for every even n, due to the half-wave symmetry} \quad (45)$$

$$b_n = \frac{2}{\pi}\int_{-\pi}^{\pi} f(\omega t)\,\text{sen}(n\omega t)d(\omega t), \quad \text{for odd n} \quad (46)$$

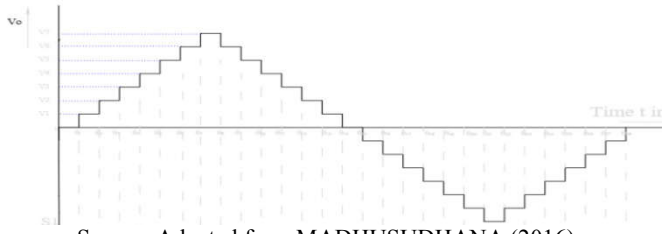

Source: Adapted from MADHUSUDHANA (2016).

Figure 7. Function with quarter-wave symmetry

Sources of Harmonics: Among the several equipments used with the objective of improving the electric power performance, such as power supplies, power controllers, among others. The main sources that generate harmonics are: Transformers with non-linear magnetization, arc devices and frequency converters, are described in more detail below.

Transformer with non-linear magnetization: When a transformer works with values exceeding the power it was designed for (this occurs at peak times) and when the voltage level is above that specified, the transformer goes into saturation. In saturation the transformer will produce a non-linear magnetizing current loaded with odd harmonics, among them the one that stands out the most is the third between the 3rd, 9th, 15th, and so on. The harmonic current will be higher when load increase occurs (DAS, 2015).

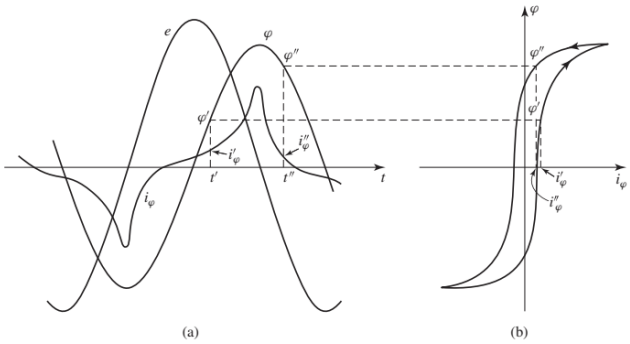

Source: UMANS (2014)

Figure 8. Waveform in the excitation phenomenon. (a) waveform of the voltage, flux in the core, and excitation current; (b) corresponding hysteresis plot

Figure 8 shows the graph of the magnetic flux (φ) with the transformer at saturation, the magnetization current (iφ) of the core material and the graph φ x iφ, which forms a hysteresis. The hysteresis shape proves that the current is non-sinusoidal, that is, a distorted signal. For the transformer at saturation the magnetizing current (a distorted signal) is not in symmetry compared to the peak value of the signal. For the supply voltage to have a very low distortion it is necessary that these harmonics are retained in the transformer, for this it must be connected in delta (UMANS, 2014, DAS, 2015). When the transformer is turned off, there is the possibility of a residual magnetic flux being retained inside the core. When the transformer is turned back on, the residual magnetic flux joins the flux produced by the surge currents and the combination of both can generate currents of up to three or more times the rated current at the load. This effect leads the transformer to extreme saturation levels, as a consequence magnetizing currents much higher than the rated magnetizing current. The dwell time of the magnetizing current is a function of the primary resistance, the higher the resistance the longer the duration of the magnetizing current. The transformer when taken to extreme levels of saturation will produce

higher levels of current distortion, that is harmonic production (LU *et al*., 2016, DEL VECCHIO, 2018).

Arc Devices: Arc devices, when supplied with a sinusoidal voltage, cause the current and voltage to be distorted, and thereby produce harmonics. Arc devices include arc welders and arc furnaces. In lighting they are present in mercury vapor, fluorescent, and sodium vapor lamps (DAS, 2015). The circuit of the arc device is formed by the voltage source in series the reactance that current to acceptable values. The arc when triggered the current increases and the voltage decreases and the limitation of the current depends on the impedance of the power system. For harmonic voltage the arc is characterized as the source of harmonics. While for current the arc load presents to be a harmonic source of stable current (BHONSLE and KELKAR, 2016, DHEEPANCHAKKRAVARTHY *et al*., 2019).

Frequency inverters: Frequency inverters are power electronics-based devices that have the purpose of controlling the speed of motors. These converters have high reliability, low maintenance, and save electricity. The frequency converter consists of a rectifier circuit, an intermediate circuit, and an inverter. The converters are widely used in industry, commerce, and homes, and have caused the increase of harmonics in the electrical grid, due to the operation being based on the commutation of the applied signal. This switching produces harmonics which distorts the power grid signal (LUO and YE, 2018, BOSE, 2020).

Decision Tree: Decision Tree is defined as the widely used software model or algorithm for machine learning with the function of making prediction, performing classification, tasks with multiple outputs and regression (NWULU, 2017, GÉRON, 2019). It can also be defined as a methodology that has the function of machine learning in addition to data mining and generates as output a Boolean decision from a set of information in the input (YANG, 2019). It can be defined more broadly that decision tree are procedures in the form of methodology, algorithms or software model that has the function of exploring data to find consistent values, make accuracies, classifications and machine learning; all this is accomplished through various input data information and as an answer in the output a Boolean decision. Machine learning is computational methods that integrates statistics and computer science. The goal of machine learning is to build algorithms through data coming from experience rather than receiving special instructions for the purpose of improving performance or making accurate predictions (MOHRI *et al*., 2018, CHARBUTY and ABDULAZEEZ, 2021).

The decision tree is a decision aid tool that has the structure, or graph, or shape of a tree that has a root, branches, and leaves. It has the advantage over other methods because of its ease of understanding and analyzing the data. The structure with root, branches and leaves has significance for the decision tree method. The root node is the top node of the tree, each node corresponds to a test on an attribute; the result produces a branch of the test. The result, at the end of all tests, ends in a node called a leaf (GUPTA, 2017, NWULU, 2017, SHARMA and KUMAR, 2016). The way to use the decision tree is done starting from the root node (top) where the condition is checked; if true it proceeds to a branch of the tree, for example right side, otherwise it proceeds to the left side. Thus it proceeds for each node encountered until it finds the leaf, which means it has finished the search on that branch. This procedure is used for each node of the tree and goes on until it reaches the leaves, each node in the decision tree correlates with an input information or attribute. The number of edges corresponds to the number of feasible conditions of the input attribute. The output attribute is presented at each node of the tree leaf that represents the prediction outcome; this outcome is influenced by the input attributes (NWULU, 2017, IZBICKI and DOS SANTOS, 2020). In Figure 9 a decision tree is visualized, where the circles represent the root and internal nodes; leaf nodes are represented by the rectangles. Between one node and another in the decision tree, each node is at a different level from the other. For example, the root node is at level 0 and the next node down is at level 1, and so on for all nodes. Each such level in the decision tree is called a depth (BARROS *et al*., 2015, KISS, 2019). Tests are performed on the nodes on a given attribute and the results of the analyses are found in the leaves. The branches represent the possible results of the tests and in the nodes leaves may contain continuous or class value labels, which are respectively, leaves of the regression tree or leaves of the classification tree. Models from other algorithms can also occur (BARROS *et al*., 2015, SHARMA and KUMAR, 2016).

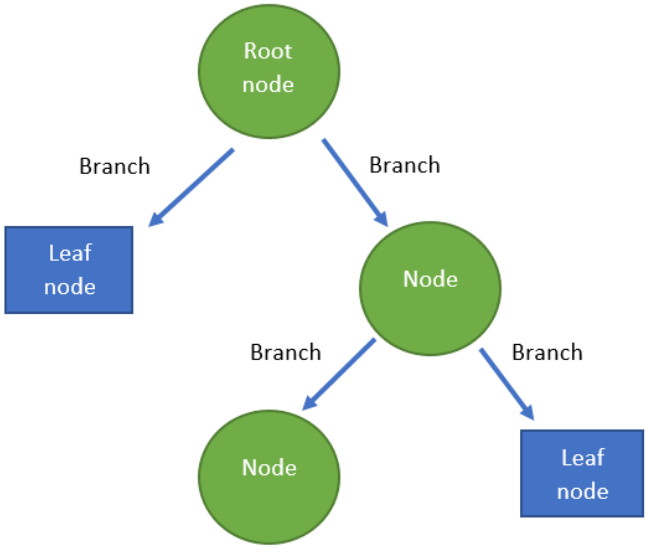

Source: Adapted from *et al*. (2015).

Figure 9. Decision Tree

Decision tree is a data mining technique, and they are of two types: classification tree and the regression tree. The classification tree is used to classify a piece of data, i.e. an object, among a predefined group of classes and uses with reference to attribute values (MAIMON and ROKACH, 2014, GUPTA, 2017). The regression tree uses a grouping of predictor variables with the goal of making the prediction of a certain dependent variable for a certain period of time. In this type of tree the prediction of the outcome can be considered a real number. As an example for the regression tree, the prediction of electricity consumption for a given day can be made for a company, given data such as location, day of the week, temperature (SHARMA and KUMAR, 2016, GUPTA, 2017). A regression tree (a type of supervised learning technique) is a prediction model, which is tree-structured, for a given numerical objective characterized by a vector of attributes that are also numerical. The regression tree is a category of decision tree, so it is trained and tested using an algorithm called the Classification and Regression Tree (CART). Using the decision tree is simple and computationally easy when creating models, since the simplicity of such models helps ensure that the regression models built are easy to interpret, thus achieving a faster response time. The regression tree works with Boolean decisions, two options for each node, with the exception of the leaf node. These Boolean decisions have splitting power that occurs through the Information Gain that to be determined depends on knowing the Entropy value. In Equation 47 and presented the equation of Information Gain (GUPTA, 2017, YANG, 2019, CHARBUTY and ABDULAZEEZ, 2021).

$$Gain(D, A) = Entropia(D) - \sum_{j=1}^{v} \frac{|D_j|}{|D|} . Entropia\ (D_j) \qquad (47)$$

From the equation we can highlight:

(D): as a given data partition;
(A): the Attributes of the set;
(V): are the distinct values (v) of an attribute (A) of the partition, that is, the number of subsets;

The Information Gain is reduced through the Entropy as can be seen in Equation 47. The calculation to find the Entropy of a binary partition is presented in Equation 48.

$$Entropia(D) = -\sum_{i=1}^{c} P_i . log_2(P_i) \quad (48)$$

In the Entropy equation we have: Pi, is the probability of the subset sample; is ratio between the number of subset sample and total value of the attribute. In the Entropy due to the division of the attributes being of binary form, in equation 48 is presented the function formed by the logarithm in base 2. Entropy is the measure of uncertainty related to a random variable. The greater the uncertainty the greater the Entropy, that is, it has a high degree of randomness; the smaller the uncertainty the lower the Entropy, that is, the attributes are more similar or close. The limit of the Entropy values is between zero (0), the minimum, and one (1) the maximum. A data partition (D) is divided into several subsets, {D1, D2, ..., Dj}, each of these subsets has a binary division that has the result aj of Attribute (A). For the selection of which partition will be used as the Root Node, for the first moment of the regression tree construction, the Information Gain is used and the selection is made by its higher value. The same occurs for the choice of the other partitions that will be linked below the root node. All these procedures will occur until reaching the leaf node; the continuation of the partitions ceases when each branch has high Entropy, that is, close or equal to 1 (GUPTA, 2017, YANG, 2019, CHARBUTY and ABDULAZEEZ, 2021).

MATERIALS AND METHODS

The proposed methodology is based on the realization of a data correlation analysis, using the decision tree technique. Through this technique a regression tree model is obtained in order to describe the existing relation between the harmonic current of a non-linear load (harmonic current generator source) and the harmonic voltage at the PCC of the electrical grid that is being analyzed. With the regression tree a better diagnosis of the influence of the non-linear load on the voltage harmonic distortion level of the point under analysis is obtained. This model is built based on the effective (rms) value measurements of harmonic voltages and currents obtained in the field, with power quality analyzers. These analyzers have current and voltage transducers which are connected to the system; these measurements and the interval between them have great influence on the construction of the regression models. The equipment used to perform the field measurement campaigns was the power quality analyzer HIOKI MODEL PW3198, which will be explained in more detail in later sub-topics. The technique used in the methodology of this work is the decision tree technique, which has as a characteristic the construction of non-parametric models of easy interpretation and data analysis. The regression models resulting from the application of the regression tree technique on the measured harmonic voltages and currents were built through the AAQEE software, which will be discussed in the next subtopic. The methodology consists of analyzing the harmonic impacts both qualitatively and quantitatively. The qualitative analysis alone is not enough, it is necessary to quantify the harmonic contribution of each customer or feeder of the analyzed electrical system. Probably every customer or feeder in the analyzed electrical system presented a contribution to the harmonic voltage distortions at the point or bar of the analyzed electrical system. The technique used was applied in a case study in such a way as to show the validity of its application in solving problems that seek to investigate the dependency relationship between two variables.

Software Aaqee: The AAQEE software is a dedicated power quality (QEE) analysis tool capable of estimating the degree of individual harmonic impact of industrial consumers on power distribution networks. The software uses simultaneous measurements of harmonic voltages, currents and powers, as well as computational intelligence techniques. Through it it is possible to perform graphical analysis of the data of electrical quantities obtained from measurement campaigns by QEE analyzers. The calculations of the QEE indicators are performed through the information established by the PRODIST norms, as well as the calculations of harmonic impacts caused by the consumer units in the distribution network of the concessionaire.

Hioki pw 3198 Power Quality Analyzer: The PW3198 power quality analyzer is an analytical instrument for monitoring and recording anomalies in the electrical power supply, allowing you to quickly investigate the causes. This equipment can be applied to analyze problems during the electric power supply, such as: voltage drop, fluctuations, harmonics, etc. The characteristics of PW3198 equipment are the following: (a) It has class A complying with IEC 61000-4-30 standard; (b) It performs high frequency transient overvoltage measurements of maximum 6 kV peak with sampling rate of minimum 1MHz; (c) Measurement and recording of harmonic and interharmonic voltage and current according to IEC 610004-7 and with minimum sampling rate of 256 samples/cycle; (d) Measurement and recording of phase angles of harmonic and interharmonic voltage and current; (e) Measurement of harmonic powers and power factor; (f) Flicker measurement according to IEC 61000-4-15; (g) Inrush current measurement; (h) Measurement of sags, swells and interruptions; (i) Mass memory of at least 2 GB; (j) Three current sensors in the range (approx.): 1A to 100 A; (l) Three flexible current sensors in the range: 200 A to 5000 A.

Flowchart: The stages of the research as shown in the flowchart in Figure 10 define the steps to be followed according to the methodology adopted for this research.

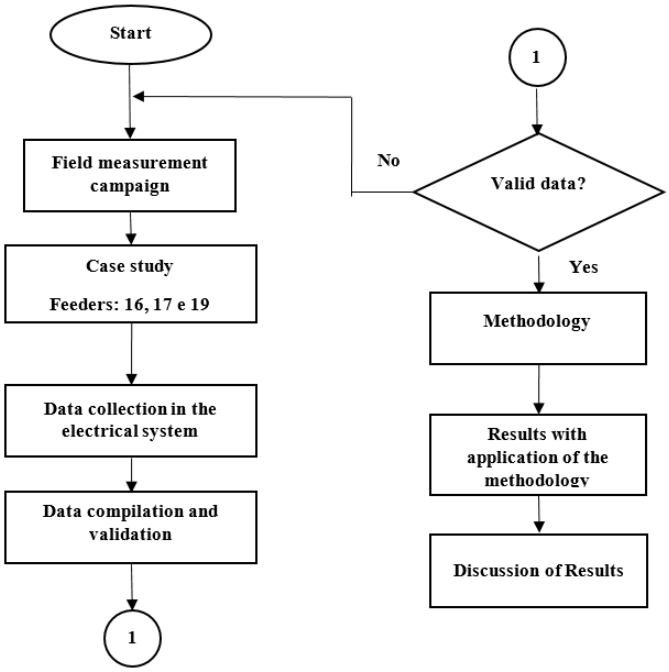

Source: Authors, (2021).

Figure 10. Flowchart of the research

RESULTS AND DISCUSSION

The case study was performed in the electrical system of an electric power utility company, which name will not be mentioned for ethical reasons. A study was carried out in three feeders and one bus of the electrical system in order to determine the influence of some non-linear loads in the harmonic distortion of the bus voltage under study, as shown in Figure 11.

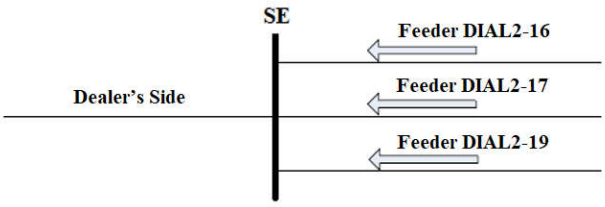

Source: Authors, (2021)

Figure 11. Identification of the harmonic impact of each feeder on a common bus in a substation

During the study in the system, measurements of harmonic voltages and currents were obtained at strategic points of the system, which allowed the construction of regression models that present the existing relationship between these quantities. The analyses were performed through a field measurement campaign carried out from May 15, 2017 to May 22, 2017 in a 13.8 kV voltage level substation of the Industrial District, in which four HIOKI PW 3198 model QEE analyzers were installed to perform simultaneous measurements in the following measurement points: transformer DITF4-04; and feeders DIAL2-16, DIAL2-17, and DIAL2-19. The objective of the installation of the QEE analyzer in the DITF4-04 transformer is to monitor the harmonic voltage at the DIBR2-03 bar (transformer output). These analyses sought to evaluate the existing correlation between order 3a harmonic currents of feeders DIAL2-16, DIAL2-17 and DIAL2-19, and the same order harmonic voltages at the DIBR2-03 (13.8 kV) bar of this substation, thus covering the zero sequence (3rd order). These feeders serve companies that have large amounts of non-linear loads installed, such as CNC machines, electric arc furnaces, plastic and aluminum injecting machines and others, therefore, large sources of harmonics. The case study presents the harmonic impact between the order 3a harmonic current of feeders DIAL2-16, DIAL2-17 and DIAL2-19 and the same order harmonic voltage of the DIBR2-03 bar.

Harmonic impact of feeders dial2-16, dial2-17 and dial2-19 on the 3rd order harmonic voltage distortion in phase a, at bar dibr2-03 of the 13.8 kv substation of di

This case study evaluates the contribution of the 3rd order harmonic currents (in phase A) produced by feeders DIAL2-16, DIAL2-17 and DIAL2-19, all served at 13.8 KV, in the 3rd order harmonic voltage distortion (phase A) at the 13.8 KV substation. Figure 12 illustrates the measurements of DIBR2-03, DIAL2-16, DIAL2-17 and DIAL2-19. It can be seen that the behavior of the DIBR2-03 voltage has great similarity to the behavior of the harmonic currents of the feeders.

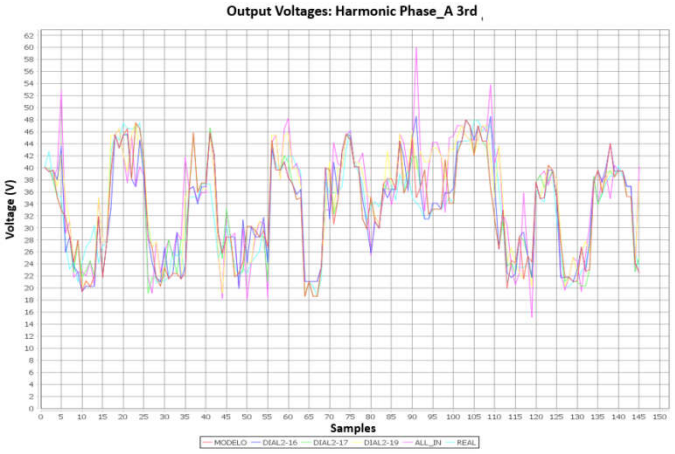

Fonte: Autores, (2021).

Figure 12 - 3rd order harmonic voltage (phase A) at the 13.8 KV industrial district substation and 3rd order harmonic currents phase A (I3_DIAL2-16, I3_DIAL2-17 and I3_DIAL2-19) at feeders DIAL2-16, DIAL2-17 and DIAL2-19, respectively

To assist in the analysis of the harmonic contribution, a regression tree model was built from a database with attributes coming from the measurements of DIBR2-03, DIAL2-16, DIAL2-17 and DIAL2-19. It can be observed that the root node of the regression tree is the attribute I3_DIAL2-19, 3rd order harmonic current of feeder DIAL2-19 (see figure 13), i.e., I3_DIAL2-19 has higher correlation with THD at DIBR2-03. Because the decision tree created by the data mining software is quite large (see Figure 13), we chose five subtrees (see Figure 14) that are capable of generalizing the knowledge gained from using the technique employed to evaluate the data. The right branch of the regression tree is shown in Figure 13. It can be seen, in the right branch of the tree, that the attribute of the node subsequent to that of the root node remains I3_DIAL2-19, when I3_DIAL2-19 is greater than 1.3 A, which evidences its greater contribution in the voltage distortion at the DIBR2-03 bar when compared to the currents I3_DIAL2-16 and I3_DIAL2-17. It can be observed in Figure 14, that the increase of the current I3_DIAL2-16 causes the reduction of THD at the DIBR2-03 bar, for the range of 2.13 A ≤I3_DIAL2-19< 2.13 A, which characterizes a cancellation of the harmonic currents. The highest value of voltage distortion (h=3) occurs when I3_DIAL2-19< 2.13 A.

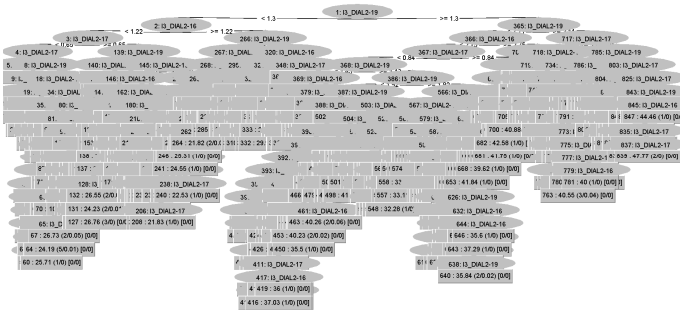

Source: Authors, (2021).

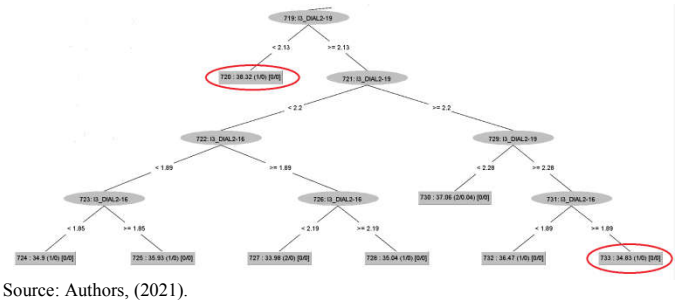

Source: Authors, (2021).

Figure 14. Right branch coming from the root node of the case study regression tree for phase A

Regression tree rules for phase A:

| | | if I3_DIAL2-19 < 2.13: 38.32 (1/0) [0/0]
| | | if I3_DIAL2-19 >= 2.13
| | | | if I3_DIAL2-19 < 2.2
| | | | | if I3_DIAL2-16 < 1.89
| | | | | | if I3_DIAL2-16 < 1.85: 34.9 (1/0) [0/0]
| | | | | | if I3_DIAL2-16 >= 1.85: 35.93 (1/0) [0/0]
| | | | | if I3_DIAL2-16 >= 1.89
| | | | | | if I3_DIAL2-16 < 2.19: 33.98 (2/0) [0/0]
| | | | | | if I3_DIAL2-16 >= 2.19: 35.04 (1/0) [0/0]
| | | | if I3_DIAL2-19 >= 2.2
| | | | | if I3_DIAL2-19 < 2.28: 37.06 (2/0.04) [0/0]
| | | | | if I3_DIAL2-19 >= 2.28
| | | | | | if I3_DIAL2-16 < 1.89: 36.47 (1/0) [0/0]
| | | | | | if I3_DIAL2-16 >= 1.89: 34.83 (1/0) [0/0]

Harmonic impact of dial2-16, dial2-17 and dial2-19 feeders on the third order harmonic voltage distortion in phase b, on dibr2-03 bar of the 13.8 kv substation of di

This study evaluates the contribution of the 3rd order harmonic currents (phase B) produced by feeders DIAL2-16, DIAL2-17 and DIAL2-19, all served at 13.8 kV, in the 3rd order harmonic voltage distortion (phase B) at the 13.8 kV substation. Figure 15 illustrates the measurements of DIBR2-03, DIAL2-16, DIAL2-17 and DIAL2-19. It can be seen that the behavior of the DIBR2-03 voltage has great similarity to the behavior of the harmonic currents of the feeders.

To assist in the analysis of the harmonic contribution, a regression tree model was built from a database with attributes coming from the measurements of DIBR2-03, DIAL2-16, DIAL2-17 and DIAL2-19. It can be observed that the root node of the regression tree is the attribute I3_DIAL2-16, 3rd order harmonic current of feeder DIAL2-16 (see Figure 16), i.e., I3_DIAL2-16 has higher correlation with THD at DIBR2-03.

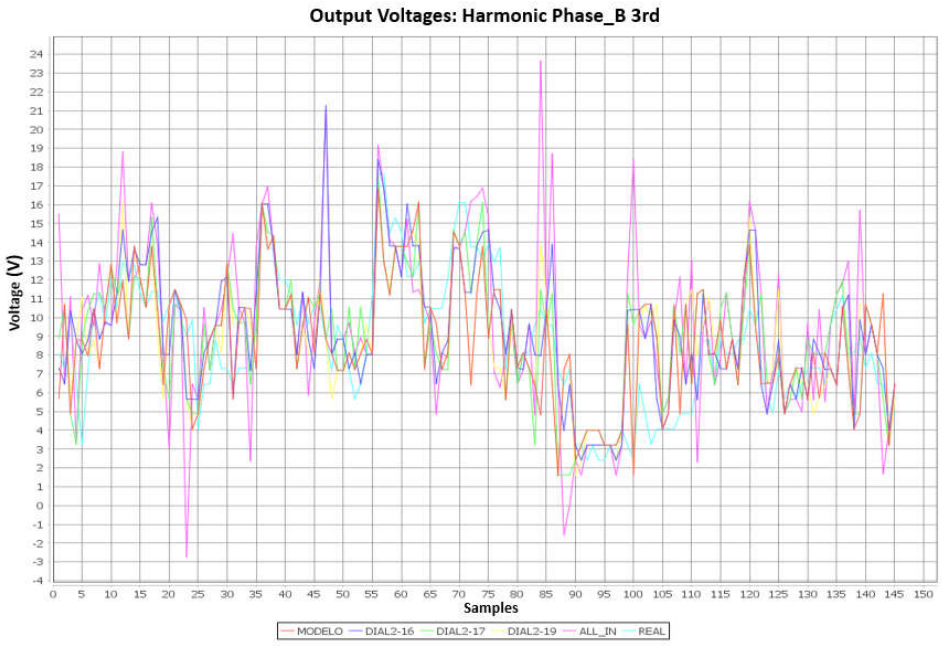

Source: Authors, (2021).

Figure 15. 3rd order harmonic voltage (phase B) at the 13.8 kV industrial district substation and 3rd order harmonic currents phase B (I3_DIAL2-16, I3_DIAL2-17 and I3_DIAL2-19) at feeders DIAL2-16, DIAL2-17 and DIAL2-19, respectively

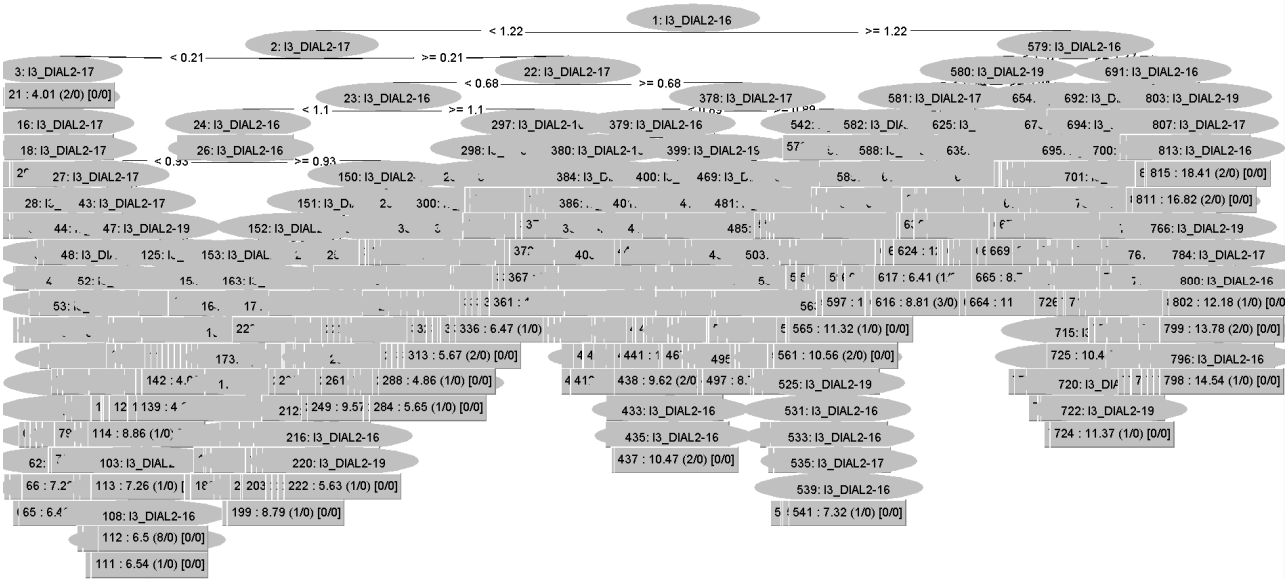

Source: Authors, (2021).

Figure 16. Case study regression tree for phase B

Because the decision tree created by the data mining software is quite large (see figure 16), we chose five subtrees (see figure 17) that are capable of generalizing the knowledge gained from using the technique employed to evaluate the data. The right branch of the regression tree is shown in Figure 16. It can be seen in the right branch of the tree that the attribute of the node subsequent to that of the root node remains I3_DIAL2-16. For Figure 17 when I3_DIAL2-16 is greater than 1.24 A, it evidences its greater contribution to voltage distortion at the DIBR2-03 bar when compared to the currents I3_DIAL2-17 and I3_DIAL2-19. It can be observed in Figure 17, that the increase of the currents I3_DIAL2-19 and I3_DIAL2-17 causes the reduction of THD at the DIBR2-03 bar, for the range of 1.24 A ≤I3_DIAL2-16< 1.24 A, which characterizes a cancellation of the harmonic currents. The highest value of voltage distortion (h=3) occurs when I3_DIAL2-16< 1.24 A.

Case study regression tree rules for phase B:

| | | | | if I3_DIAL2-16 < 1.24 : 13.8 (2/0.01) [0/0]
| | | | | if I3_DIAL2-16 >= 1.24
| | | | | | if I3_DIAL2-16 < 1.3
| | | | | | | if I3_DIAL2-19 < 1
| | | | | | | | if I3_DIAL2-19 < 1
| | | | | | | | | if I3_DIAL2-17 < 0.5 : 10.42 (1/0) [0/0]
| | | | | | | | | |if I3_DIAL2-17 >= 0.5 : 11.45 (2/0) [0/0]
| | | | | | | | if I3_DIAL2-19 >= 1 : 8.78 (1/0) [0/0]
| | | | | | | if I3_DIAL2-19 >= 1 : 12.97 (1/0) [0/0]
| | | | | | if I3_DIAL2-16 >= 1.3
| | | | | | | if I3_DIAL2-16 < 1.32 : 13.04 (1/0) [0/0]
| | | | | | | if I3_DIAL2-16 >= 1.32 : 12.1 (1/0) [0/0]

Harmonic impact of feeders dial2-16, dial2-17 and dial2-19 on the 3rd order harmonic voltage distortion in phase c, at bar dibr2-03 of the 13.8 kv substation of di: This case study evaluates the contribution of the 3rd order (phase C) harmonic currents produced by feeders DIAL2-16, DIAL2-17 and DIAL2-19, all served at 13.8 kV, in the 3rd order (phase C) harmonic voltage distortion at the 13.8 kV substation. Figure 18 illustrates the measurements of DIBR2-03, DIAL2-16, DIAL2-17 and DIAL2-19.

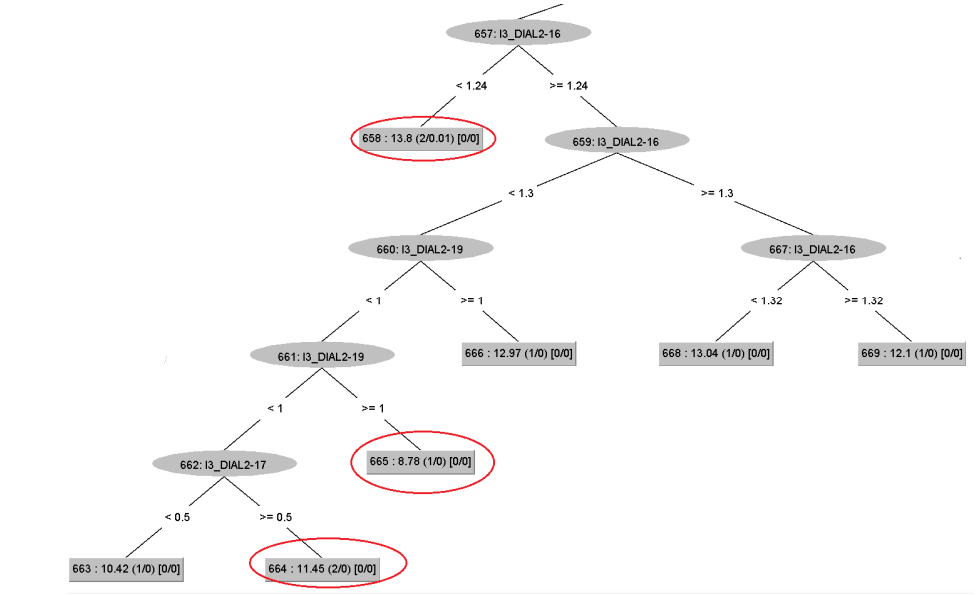

Source: Authors, (2021).

Figure 17. Right branch coming from the root node of the case study regression tree for phase B

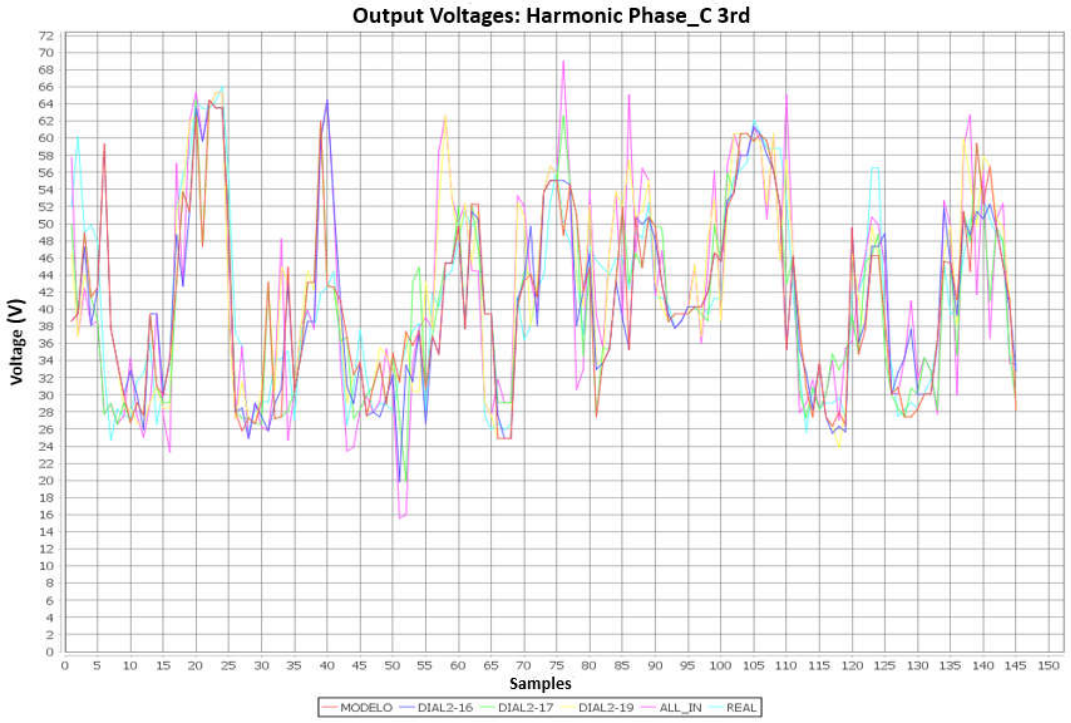

Source: Authors, (2021).

Figure 18 - 3rd order harmonic voltage (phase C) at the 13.8 kV industrial district substation and 3rd order harmonic currents phase C (I3_DIAL2-16, I3_DIAL2-17 and I3_DIAL2-19) at feeders DIAL2-16, DIAL2-17 and DIAL2-19, respectively

It can be seen that the behavior of the DIBR2-03 voltage has great similarity to the behavior of the harmonic currents of the feeders. To assist in the analysis of the harmonic contribution, a regression tree model was built from a database with attributes coming from the measurements of DIBR2-03, DIAL2-16, DIAL2-17 and DIAL2-19. It can be observed that the root node of the regression tree is the attribute I3_DIAL2-17, 3rd order harmonic current of feeder DIAL2-17 (see figure 19), i.e., I3_DIAL2-17 has higher correlation with THD at DIBR2-03. Because the decision tree created by the data mining software is quite large (see Figure 19), we chose six subtrees (see Figure 20) that are capable of generalizing the knowledge gained from using the technique employed to evaluate the data. The right branch of the regression tree is shown in Figure 20. Note that in this case, other variables also influence the voltage distortion at the DIBR2-03 bar. The highest value of voltage distortion (h=3) occurs when I3_DIAL2-17 < 1.34 A, I3_DIAL2-17 ≥ 1.26 A, I3_DIAL2-16 < 1.86 A and I3_DIAL2-17 < 1.27 A.

On the other hand, the lowest value of the 3rd order harmonic voltage occurs when I3_DIAL2-17 ≥ 1.34 A.

Case study regression tree rules for phase C:

```
| | | | | | | | | | if  I3_DIAL2-17 < 1.34
| | | | | | | | | | | if  I3_DIAL2-17 < 1.26: 27.49 (1/0) [0/0]
| | | | | | | | | | | if  I3_DIAL2-17 >= 1.26
| | | | | | | | | | | | if  I3_DIAL2-16 < 1.86
| | | | | | | | | | | | | if  I3_DIAL2-17 < 1.27: 31.71 (1/0) [0/0]
| | | | | | | | | | | | | if  I3_DIAL2-17 >= 1.27
| | | | | | | | | | | | | | if  I3_DIAL2-16 < 1.52: 29.67 (1/0) [0/0]
| | | | | | | | | | | | | | if  I3_DIAL2-16 >= 1.52: 30.59 (1/0) [0/0]
| | | | | | | | | | | | if I3_DIAL2-16 >= 1.86
| | | | | | | | | | | | if  I3_DIAL2-16 < 1.93
| | | | | | | | | | | | | if  I3_DIAL2-19 < 0.96: 27.38 (1/0) [0/0]
| | | | | | | | | | | | | if  I3_DIAL2-19 >= 0.96: 28.32 (3/0) [0/0]
| | | | | | | | | | | | if  I3_DIAL2-16 >= 1.93: 30.08 (2/0) [0/0]
```

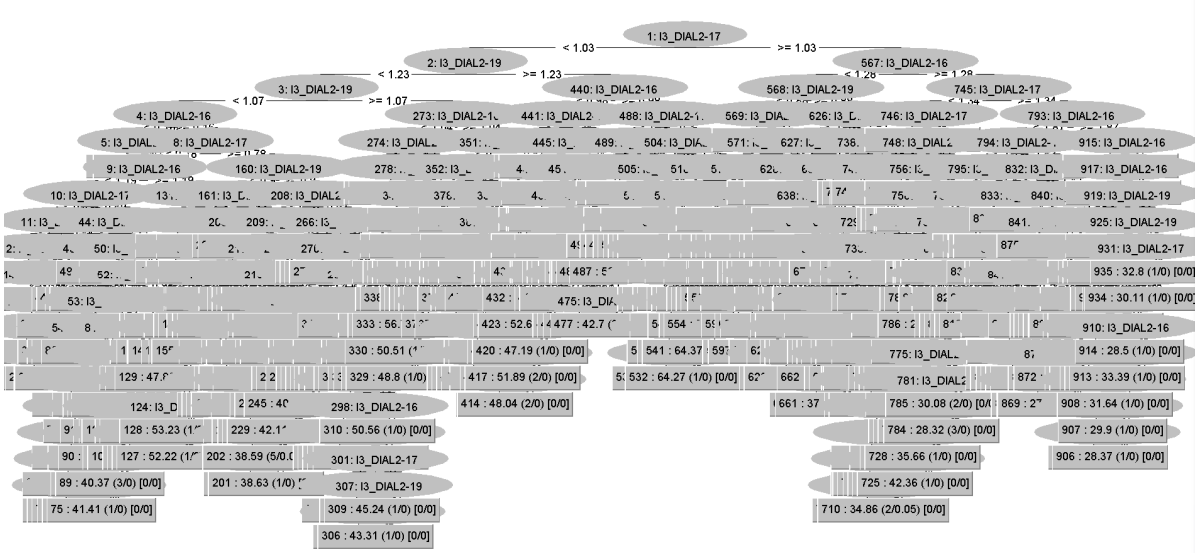

Source: Authors, (2021).

Figure 19. Case study regression tree for phase C

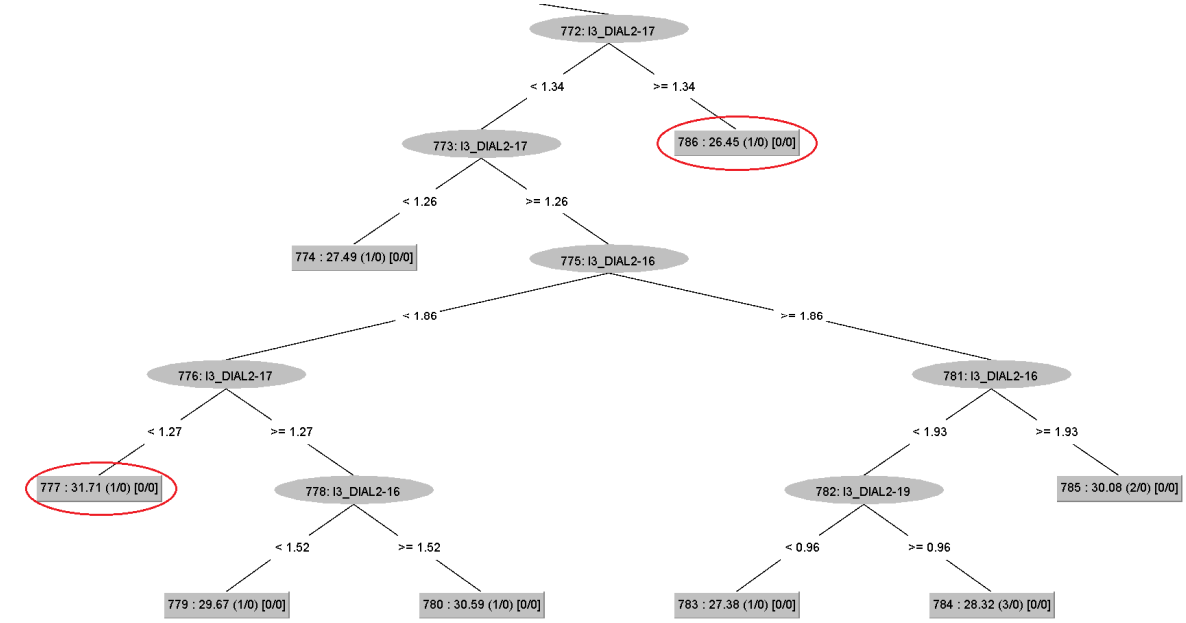

Source: Authors, (2021).

Figure 20. Right branch coming from the root node of the case study regression tree for phase C

DISCUSSION OF RESULTS

In this study it was analyzed the contribution of feeders DIAL2-16, DIAL2-17 and DIAL2-19 to the increase of harmonic voltage distortion at the DIBR2-03 bar for 3rd harmonic order in phases A, B and C. During the analysis of the results provided by the application of the decision tree technique it was found that phase A of feeder DIAL2-19, phase B of feeder DIAL2-16 and phase C of feeder DIAL2-17 have higher contribution in harmonic voltage distortion at the DIBR2-03 bar when compared to the results of phases B and C of feeder DIAL2-19, phases A and C of feeder DIAL2-17.

Table 1. Harmonic Impact Factor for 3rd order (%) MAE

BASE	PHASE A	PHASE B	PHASE C
DIAL2-16	30,366	36,407	23,660
DIAL2-17	16,017	25,852	26,434
DIAL2-19	43,587	15,507	36,422
BACKGROUND	10,030	22,233	13,484

Soucer: Authors, (2021).

Table 1 presents the impact factor of the 3rd harmonic, through the mean absolute error - MAE (given in percentage) of the three phases for each feeder, including the background which are the other feeders not measured.

Feeder DIAL2-19 contributed the impact factor in the 3rd harmonic for phase A with 43.587%. Feeder DIAL2-16 contributed with impact factor 36.407% for phase B. For phase C feeder DIAL2-17 contributed with impact factor 26.434%. These were the feeders that contributed the most to the increase in harmonic voltage distortion at the DIBR2-03 bar for 3rd harmonic order in phases A, B and C (DIAL2-19, DIAL2-16 and DIAL2-17, respectively). This result enables better decision making in power system management, i.e., directing the actions to treat harmonic impacts caused by nonlinear loads first to the phases and feeders that cause the greatest impacts.

CONCLUSIONS

A measurement campaign was conducted to collect data on harmonic levels in the three feeders of the electric system studied, during a period of seven days in accordance with module 8 of PRODIST 2021. With the collected data it was possible to make a correlation analysis between the 3rd order harmonic currents injected into the feeders and the voltage distortion at the bar of the studied electrical system through the decision tree technique. With these analyses, it was created a profile of the feeders DIAL2-16, DIAL2-17 and DIAL2-19 in the 3rd harmonic order, to then mitigate the harmonic voltage

distortion at the DIBR2-03 bar under study, caused by the impacts of the harmonic currents of these feeders. A report of the analyses performed of the harmonic impacts was described, that it serves as a diagnostic document of the measured points; thus obtaining a better management of the electric system, promoting the inclusion in the electric energy tariff of the implications of the harmonic content injected in the electric system. In this way, this study presented and applied in practice, actions for the analysis of harmonic impacts in electrical power distribution systems through the demonstration of the decision tree model. With the results obtained, it became evident the efficiency of the application of the developed methodology for the analysis of harmonic impacts on electrical grids caused by non-linear loads, through the Decision Tree technique. For future works it is suggested: the application of the same developed methodology to identify which non-linear loads contribute to harmonic voltage distortions on the analyzed feeders; the application of other statistical techniques such as Neural and Fuzzy Networks; to investigate the influence of harmonic distortion on the power factor; application of active and passive filters on the analyzed feeders to treat the harmonic voltage distortion problem.

Acknowledgments: To the Post Graduate Program Master in Process Engineering of the Institute of Technology of the Federal University of Pará (PPGEP/ITEC/UFPA) and the Institute of Technology and Galileo Education of the Amazon (ITEGAM) for their research support.

REFERENCES

AGÊNCIA NACIONAL DE ENERGIA ELÉTRICA–ANEEL. Procedimentos de Distribuição de Energia Elétrica no Sistema Elétrico Nacional–PRODIST: Módulo 8–Qualidade da Energia Elétrica. 2018.

ALEXANDER, S. *et al*. Development of solar photovoltaic inverter with reduced harmonic distortions suitable for Indian sub-continent. Renewable and Sustainable Energy Reviews, v. 56, n. C, p. 694-704, 2016.

ALMEIDA, Lucas Rodrigues de *et al*. Modelagem para análise de desempenho de fornos micro-ondas no contexto da qualidade de energia elétrica. 2016.

ALMEIDA, RIVANILDO DUARTE; LEITE, JANDECY CABRAL. Análise de Impactos Harmônicos em Redes Elétricas de Média Tensão. 1. ed., v. 2. 125p, Novas Edições Acadêmicas, Alemanha, 2018.

BARROS, Rodrigo C.; DE CARVALHO, André CPLF; FREITAS, Alex A. Automatic design of decision-tree induction algorithms. Springer, 2015.

BAYINDIR, Ramazan *et al*. Smart grid technologies and applications. Renewable and sustainable energy reviews, v. 66, p. 499-516, 2016.

BECKER, L. R.; DIAS, J. B.; PILLOT, B. D. F. Análise experimental de uma microrrede fotovoltaica isolada e conectada à rede. In: Conferência Internacional de Energias Inteligentes. CIEI&EXPO 2016, Curitiba-PR, Brasil, 16-18 novembro, 2016.

BELE, Shraddha; GHUTKE, Pratik. Generalized Unified Power Quality Conditioner (UPQC) System with an Improved Control Method Under Distorted and Unbalanced Load Conditions. 2019.

BELEIU, Horia Gheorghe *et al*. Management of power quality issues from an economic point of view. Sustainability, v. 10, n. 7, p. 2326, 2018.

BELTRAN-CARBAJAL, F.; SILVA-NAVARRO, G. A fast parametric estimation approach of signals with multiple frequency harmonics. Electric Power Systems Research, v. 144, p. 157-162, 2017.

BHONSLE, Deepak C.; KELKAR, Ramesh B. Analyzing power quality issues in electric arc furnace by modeling. Energy, v. 115, p. 830-839, 2016.

BOSE, Bimal K. Power electronics and motor drives: advances and trends. Academic press, 2020.

CARDOSO JR, Ricardo Abranches Felix; HOFFMANN, Alessandra Schwertner. Environmental licensing for transmission systems and electricity sector planning in Brazil. Energy Policy, v. 132, p. 1155-1162, 2019.

CARVALHO, Thaisa Luup Cabral. Estudo das harmônicas geradas internamente em motores elétricos assíncronos trifásicos. 2018.

CHAKRAVORTY, Diptargha *et al*. Impact of modern electronic equipment on the assessment of network harmonic impedance. IEEE Transactions on Smart Grid, v. 8, n. 1, p. 382-390, 2016.

CHARBUTY, Bahzad; ABDULAZEEZ, Adnan. Classification based on decision tree algorithm for machine learning. Journal of Applied Science and Technology Trends, v. 2, n. 01, p. 20-28, 2021.

DA SILVEIRA, Lucas C.; BERNARDON, Daniel P.; RADUNS, Caroline. Elaboration of an impact study on the medium voltage electrical system caused by nonlinear loads. In: 2018 Simposio Brasileiro de Sistemas Eletricos (SBSE). IEEE, 2018. p. 1-6.

DAS, J. C. Power system harmonics and passive filter designs. John Wiley & Sons, 2015.

DE LEON II, John Diaz; LIEBLICK, Bryan; WILIE, Edward. How facts on the distribution system are being used to improve power quality. CIRED-Open Access Proceedings Journal, v. 2017, n. 1, p. 691-694, 2017.

DEL VECCHIO, Robert M. *et al*. Transformer design principles. Third edition. CRC press, 2018.

DESAI, J. V.; DADHICH, Pradeep Kumar; BHATT, P. K. Investigations on harmonics in smart distribution grid with solar PV integration. Technology and Economics of Smart Grids and Sustainable Energy, v. 1, n. 1, p. 11, 2016.

DHANDE, Neha; PATHAN, Ms Nagmanaj. UPQC System for Improved Control Method. framework, v. 6, n. 03, 2019.

DHEEPANCHAKKRAVARTHY, Azhagesan; SELVAN, Manickavasagam Parvathy; MOORTHI, Sridharan. Alleviation of power quality issues caused by electric arc furnace load in power distribution system using 3-phase four-leg DSTATCOM. Journal of The Institution of Engineers (India): Series B, v. 100, n. 1, p. 9-22, 2019.

DIONISIO, Guilherme; SPALDING, Luiz Eduardo Schardong. Visualização da forma de onda e conteúdo harmônico da corrente elétrica alternada em eletrodomésticos. Revista Brasileira de Ensino de Física, v. 39, 2016.

FORTES, Rárison Roberto Acácio. Propagação de harmônicas produzidas por inversores fotovoltaicos e transformadores assimetricamente magnetizados na geração distribuída. 2018.

FRANCHI, Thiago Prini. Fluxo de potência trifásico harmônico baseado no método backward/forward sweep para o estudo dos harmônicos gerados por cargas industriais e residenciais. 2017.

GÉRON, Aurélien. Mãos à Obra: Aprendizado de Máquina com Scikit-Learn & TensorFlow. Alta Books, 2019.

GOPAL, M. Rama; YARNAGULA, Sobharani. Simulation and analysis of shuntActive power filter for power quality improvement. international journal Of advanced trends in computer science and Engineering, v. 3, n. 1, p. 26-31, 2014.

GUPTA, Bhumika *et al*. Analysis of various decision tree algorithms for classification in data mining. International Journal of Computer Applications, v. 163, n. 8, p. 15-19, 2017.

HALLIDAY, D.; RESNICK, R.; WALKER, J. Fundamentos de física: gravitação, ondas e termodinâmica. 10ª edição ed. Rio de Janeiro: LTC, 2016. v. 2.

IEC TR 61000-3-6:2008. Electromagnetic compatibility (EMC) - Part 3-6: Limits - Assessment of emission limits for the connection of distorting installations to MV, HV and EHV power systems.

IEEE STANDARD 519□2014. IEEE recommended practices and requirements for harmonic control in electrical powersystems. 2014.

IEEE Std 1453-2015. IEEE Recommended Practice for the Analysis of Fluctuating Installations on Power Systems, 2015.

IEEE-1159. IEEE recommended practice for monitoring electric power quality. IEEE Std 1159-2019, v. 99, p. 1–98, 2019.

IZBICKI, Rafael; DOS SANTOS, Tiago Mendonça. Aprendizado de máquina: uma abordagem estatística. Rafael Izbicki, 2020.

JAISIVA, S.; NEELAN, S.; ILANSEZHIAN, T. Harmonic analysis in non–linear loads of power system. International Research Journal of Engineering and Technology (IRJET), v. 3, n. 05, p. 1474-1478, 2016.

JAYASINGHE, Shantha Gamini *et al*. Review of ship microgrids: System architectures, storage technologies and power quality aspects. inventions, v. 2, n. 1, p. 4, 2017.

JEDRZEJCZAK, Jakub *et al*. Reliability assessment of protective relays in harmonic-polluted power systems. IEEE Transactions on Power Delivery, v. 32, n. 1, p. 556-564, 2016.

JOHNSON, Daniel Ogheneovo; HASSAN, Kabiru Alani. Issues of power quality in electrical systems. International Journal of Energy and Power Engineering, v. 5, n. 4, p. 148-154, 2016.

KAMEL, Khechiba; LAID, Zellouma; ABDALLAH, Kouzou. Mitigation of harmonics current using different control algorithms of shunt active power filter for non-linear loads. In: 2018 International Conference on Applied Smart Systems (ICASS). IEEE, 2018. p. 1-4.

KAVITHA, V.; SUBRAMANIAN, K. Investigation of power quality issues and its solution for distributed power system. In: 2017 International Conference on Circuit, Power and Computing Technologies (ICCPCT). IEEE, 2017. p. 1-6.

KERBER, Carlos MM; ESTEVES, Cláudio A. Série harmônica e suas representações gráficas: análise de padrões e sugestões. In: 70ª Reunião Anual da SBPC, UFAL, Maceió – AL, Brasil, 22 a 28 de julho, 2018.

KISS, Ágnes *et al*. Sok: Modular and efficient private decision tree evaluation. Proceedings on Privacy Enhancing Technologies, v. 2019, n. 2, p. 187-208, 2019.

KO, Wei-Hsiang; GU, Jyh-Cherng. Impact of shunt active harmonic filter on harmonic current distortion of voltage source inverter-fed drives. IEEE Transactions on Industry Applications, v. 52, n. 4, p. 2816-2825, 2016.

KOLMAKOV, V. O. *et al*. Analysis of dynamic characteristics of frequency-dependent links. In: IOP Conference Series: Materials Science and Engineering. IOP Publishing, 2020. p. 012026.

KULLARKAR, Vicky T.; CHANDRAKAR, Vinod K. Power quality analysis in power system with non linear load. Int. J. Electr. Eng, v. 10, p. 33-45, 2017.

KUMAR, Dinesh; ZARE, Firuz. Harmonic analysis of grid connected power electronic systems in low voltage distribution networks. IEEE Journal of Emerging and selected topics in Power Electronics, v. 4, n. 1, p. 70-79, 2015.

KUMAR, L. ASHOK AND ALEXANDER, S. ALBERT. Computational Paradigm Techniques for Enhancing Electric Power Quality, First edition, New York, NY : CRC Press/Taylor & Francis Group, 2019.

LANCZOS, Cornelius; BOYD, John. Discourse on Fourier series. Society for industrial and applied mathematics, 2016.

LOPEZ, A. *et al*. Harmonic Distortions on Grid Connected Double Fed Generator: A Review. IEEE Latin America Transactions, v. 14, n. 4, p. 1745-1751, 2016.

LU, Junwei; ZHAO, Xiaojun; YAMADA, Sotoshi. Harmonic balance finite element method: applications in nonlinear electromagnetics and power systems. John Wiley & Sons, 2016.

LUO, Fang Lin; YE, Hong. Power electronics: advanced conversion technologies. CRC press, 2018.

LV, Xiupin; LIAO, Xiaofeng; YANG, Bo. Um novo gerador de números pseudo-aleatórios de rede de mapa acoplado com atraso variável no tempo. Nonlinear Dynamics , v. 94, n. 1, pág. 325-341, 2018.

MADHUSUDHANA, J. *et al*. Genetic algorithm based 15 level modified multilevel inverter for stand alone photvoltaic applications. 2016.

MAIMON, Oded Z.; ROKACH, Lior. Data mining with decision trees: theory and applications. World scientific, 2014.

MANUSOV, Vadim Z.; KHRIPKOV, Viktor V. Comparative Analysis of Mathematical Models for the Coefficient of Conductor Resistance Increase Due to Higher Harmonics. In: 2018 XIV International Scientific-Technical Conference on Actual Problems of Electronics Instrument Engineering (APEIE). IEEE, 2018. p. 133-136.

MEYER, Jan *et al*. Assessment of prevailing harmonic current emission in public low-voltage networks. IEEE Transactions on Power Delivery, v. 32, n. 2, p. 962-970, 2016.

MIKKILI, Suresh; PANDA, Anup Kumar. Power quality issues: current harmonics. CRC press, 2018.

MILANI, Karim Roshan *et al*. Measurement and analysis of base transceiver stations power quality parameters and assessment of its unfavourable effects on Iran distribution systems. CIRED-Open Access Proceedings Journal, v. 2017, n. 1, p. 761-765, 2017.

MOHRI, Mehryar; ROSTAMIZADEH, Afshin; TALWALKAR, Ameet. Foundations of machine learning. MIT press, 2018.

MONTEIRO, Henrique LM *et al*. Harmonic impedance measurement based on short time current injections. Electric power systems research, v. 148, p. 108-116, 2017.

MOTTA, Lukas; FAÚNDES, Nicolás. Active/passive harmonic filters: Applications, challenges & trends. In: 2016 17th International Conference on Harmonics and Quality of Power (ICHQP). IEEE, 2016. p. 657-662.

NAHVI, Mahmood; EDMINISTER, Joseph A. Schaum's outline of Electric Circuits. McGraw-Hill Education, 2018.

NILSSON, James William; RIEDEL, Susan A. Electric circuits. Pearson Education Limited, 2020.

NWULU, Nnamdi I. A decision trees approach to oil price prediction. In: 2017 International Artificial Intelligence and Data Processing Symposium (IDAP). IEEE, 2017. p. 1-5.

OLIVEIRA, Edson Farias de *et al*. Avaliação da distorção harmônica total de tensão no ponto de acoplamento comum industrial usando o processo KDD baseado em medição. 2018.

OZDEMIR, Caner. Inverse synthetic aperture radar imaging with MATLAB algorithms. John Wiley & Sons, 2021.

PAPIČ, Igor *et al*. A Benchmark Test System to Evaluate Methods of Harmonic Contribution Determination. IEEE Transactions on Power Delivery, v. 34, n. 1, p. 23-31, 2018.

PATEL, Nirav; GUPTA, Nitin; BANSAL, Ramesh C. Combined active power sharing and grid current distortion enhancement□based approach for grid□connected multifunctional photovoltaic inverter. International Transactions on Electrical Energy Systems, v. 30, n. 3, p. e12236, 2020.

RANI, R. Sheba; RAO, C. Srinivasa; KUMAR, M. Vijaya. Analysis of active power filter for harmonic mitigation in distribution system. In: 2016 International Conference on Electrical, Electronics, and Optimization Techniques (ICEEOT). IEEE, 2016. p. 1338-1446.

RASUL, Mohamed JMA; KHANG, H. V.; KOLHE, Mohan. Harmonic mitigation of a grid-connected photovoltaic system using shunt active filter. In: 2017 20th International Conference on Electrical Machines and Systems (ICEMS). IEEE, 2017. p. 1-5.

SAAD, Hani *et al*. On resonances and harmonics in HVDC-MMC station connected to AC grid. IEEE Transactions on Power Delivery, v. 32, n. 3, p. 1565-1573, 2017.

SAGGIO, Giovanni. Principles of analog electronics. CRC Press, 2019.

SALEHI, Seyed Mohsen; HASANZADEH, Saeed; DEHGHAN, Seyed Mohammad. An Investigation to the Atmospheric Effects on Generating Harmonic Distortion in a Solar Farm. Journal of Solar Energy Research, v. 4, n. 3, p. 200-208, 2019.

SANG, Yong *et al*. A Novel Method of Improving Non-Sinusoidal Periodic Waveform in Force Excitation Control System. International Journal of Automation Technology, v. 10, n. 3, p. 420-428, 2016.

SEITHTANABUTARA, Varinrumpai; JOOKJANTRA, Kittichai; WONGWUTTANASATIAN, Tanakorn. Effect of different waveforms and harmonic frequency orders on bubble cavitation in dual-frequency ultrasonic intensification. Chemical Engineering and Processing-Process Intensification, v. 157, p. 108134, 2020.

SEROV, Valery *et al*. Fourier series, Fourier transform and their applications to mathematical physics. New York: Springer, 2017.

SEZGIN, Erhan; SALOR, Özgül. Analysis of power system harmonic subgroups of the electric arc furnace currents based on a hybrid time-frequency analysis method. IEEE Transactions on Industry Applications, v. 55, n. 4, p. 4398-4406, 2019.

SHARMA, Himani; KUMAR, Sunil. A survey on decision tree algorithms of classification in data mining. International Journal of Science and Research (IJSR), v. 5, n. 4, p. 2094-2097, 2016.

SILVA, E. N. M., RODRIGUES, A. B., SILVA, M. G. Estimação probabilística do nivel de distorção harmônica total de tensão em redes de distribuição secundárias. XXI Congresso Brasileiro de Automática, CBA2016, UFES, Vitória – ES, Brasil, 3-7 outubro, 2016.

SILVA, W. F. da *et al*. Análise dos impactos harmônicos na qualidade da energia elétrica utilizando kdd–estudo de caso na Universidade Federal do Pará.Belém, 2019.

SOLIMAN, SOLIMAN ABDEL-HADY AND ALAMMARI, RASHID ABDEL-KADER. Electric Power Quality Recognition and Classification in Distribution Networks, Power Quality Issues, IntechOpen, DOI: 10.5772/53081, 2013.

SOLIMAN, SOLIMAN ABDELHADY AND ALKANDARI, AHMAD MOHAMMAD. Electric Power Systems Harmonics - Identification and Measurements, Power Quality Harmonics Analysis and Real Measurements Data, Gregorio Romero Rey and Luisa Martinez Muneta, IntechOpen, DOI: 10.5772/16412, November 23rd 2011.

SOUZA, JAYNE DO NASCIMENTO; LEITE, JANDECY CABRAL; ALMEIDA, RIVANILDO DUARTE. Analysis of Harmonic Impacts on an Electric System Bus Using Artificial Neural Networks. Post-Graduation Program in Process Engineering of the Institute of Technology of the Federal University of Pará, Federal University of Pará (UFPA), Belém-Pará, Brazil, Institute of Technology and Education Galileo of the Amazon (ITEGAM), Manaus-Amazonas, Brazil, 2021.

STIEGLER, Robert *et al*. Measurement of network harmonic impedance in presence of electronic equipment. In: 2015 IEEE International Workshop on Applied Measurements for Power Systems (AMPS). IEEE, 2015. p. 49-54.

TRIPATHI, Pratibha *et al*. Application of APLC for Power Quality Improvement in Power Grid. International Journal of Master of Engineering Research and Technology, v. 3, n. 3, pp. 251 – 255, 2016.

ULLAH, ASAD; SHEIKH, INAM UL HASAN; ARSHAD, SHAHZAD; SALEEM, FAISAL. Digital Active Power Filter Controller Design for Current Harmonics in Power System, Department of Electrical Engineering, University of Engineering and Technology, Taxila Taxila, Pakistan, 2019.

UMANS, Stephen D. Máquinas Elétricas de Fitzgerald e Kingsley-7. AMGH Editora, 2014.

WANG, Yang *et al*. Characteristics of harmonic distortions in residential distribution systems. IEEE Transactions on Power Delivery, v. 32, n. 3, p. 1495-1504, 2016.

WATEGAONKAR, Suraj S.; PATIL, Swapnil S.; JADHAV, Pradnya R. Mitigation of current harmonics using shunt active power filter. In: 2018 3rd International Conference for Convergence in Technology (I2CT). IEEE, 2018. p. 1-5.

YANG, Feng-Jen. An extended idea about decision trees. In: 2019 International Conference on Computational Science and Computational Intelligence (CSCI). IEEE, 2019. p. 349-354.

YANG, Yongheng; ZHOU, Keliang; BLAABJERG, Frede. Current harmonics from single-phase grid-connected inverters—Examination and suppression. IEEE Journal of Emerging and Selected Topics in Power Electronics, v. 4, n. 1, p. 221-233, 2016.

ZOBAA, AHMED F. AND ALEEM, SHADY H. E. ABDEL. Power Quality in Future Electrical Power Systems, Published by The Institution of Engineering and Technology, London, United Kingdom, 2017.

****